Identifying Sources of Per- and Polyfluoroalkyl Substances in Photolithography Wastewater

CNF Project Number: 2938-21
Principal Investigator(s): Damian Helbling
User(s): Vie Villafuerte

Affiliation(s): Civil and Environmental Engineering, Cornell University

Primary Source(s) of Research Funding: Semiconductor Research Corporation

Contact: deh262@cornell.edu, vav27@cornell.edu

Research Group Website: https://helbling.research.engineering.cornell.edu/

Primary CNF Tools Used: Suss Gamma Resist Cluster, ASML DUV Stepper, Oxford 100 ICP Dielectric, PlasmaTherm Versaline Deep Silicon Etch

Abstract:

Per- and polyfluoroalkyl substances (PFASs) are contaminants of concern to environmental and human health.1 Organofluorine-containing chemicals are widely used in semiconductor manufacturing processes such as lithographic patterning, etching, and stripping, among others; 2however, their release from specific fabrication processes is not well understood. While previous work focused on PFASs in wastewater and photolithography materials, putative sources such as plasma etching processes and scrubber blowdown have been underexplored. This study investigated PFAS formation during plasma etching of silicon wafers using various fluorinated etch gases. We performed nine plasma etch experiments and collected aqueous blowdown samples from a plasma-wet scrubber connected to two plasma etch tools. The samples were analyzed for total fluorine (TF), adsorbable organic fluorine (AOF), and 24 target PFASs. The goal of this project was to demonstrate if plasma etching processes are a significant source of PFASs and other organofluorine compounds in semiconductor fabrication facilities (fabs) emissions.

Summary of Research:

A variety of PFASs and other organofluorine-containing compounds are used during semiconductor manufacturing, 2and emissions of PFASs from fabs are of emerging concern. While most previous studies have focused on PFASs in fab wastewater samples or specific materials used during photolithography,[3,4]other potential PFAS sources, such as plasma etching processes and air scrubber blowdown, remain underexplored.

Fluorine inputs to plasma etch processes include both organofluorine-containing materials coated on the wafers (e.g., photoresists) and fluorinated gases. Hydrofluorocarbons (HFCs) and perfluorocarbons (PFCs), commonly used for silicon wafer etching, introduce fluorine into the system. The exhaust gas from these processes is treated with wet scrubbers, where PFASs can partition into aqueous scrubber blowdown. We hypothesize that fluorine-containing gases used in plasma etch processes generate fluorine radicals that react with organic chemicals deposited on the wafer surface to form PFASs, which are then released in the exhaust, likely a key source of PFASs measured in fab effluent.

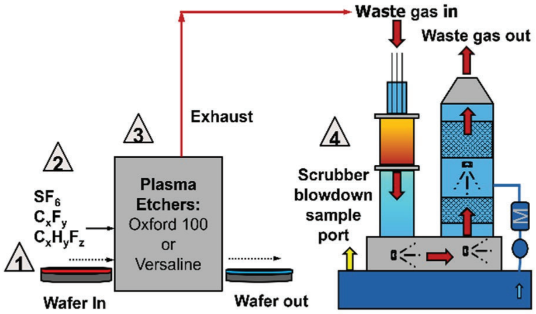

Figure 1: Schematic of the plasma etching and scrubbing process. The resulting exhaust from a plasma etch is routed to a scrubber system. Scrubber blowdown is collected for PFAS analysis.

We designed experiments to (1) demonstrate the formation of PFASs during plasma etching and transport to aqueous scrubber blowdown; and (2) identify the specific process conditions influencing PFAS formation. Four key process variables were investigated: (1) photoresist type, (2) choice of fluorinated etch gas, (3) plasma etching tool, and (4) use of plasma-enabled vs. non-plasma scrubber (Figure 1). We coated 4-inch silicon wafers with 500 nm of UV^{TM} 210 Positive DUV photoresist using the Gamma Photoresist Cluster. The ASML DUV Wafer Stepper was used for edge-bead removal. Etching experiments used six fluorinated gases including CH_2F_2, CHF_3, C_4F_8, C_4F_6, SF_6, and $C_3H_2F_4$ (a low global warming potential alternative gas that demonstrated to meet semiconductor manufacturing performance objectives). [5]The etching experiments were conducted on both bare silicon and photoresist-coated wafers in each etching tool: the PlasmaTherm Versaline Deep Silicon Etch, which uses the Bosch process, and the Oxford 100 ICP Dielectric tool, with each listed gas. Finally, duplicate blowdown samples were collected immediately after the completion of each etching experiment from the GST Durian "plasma-wet" scrubber with the plasma feature deactivated, to isolate PFAS contributions of the etching process alone. The plasma scrubber feature was activated only during the first Versaline experiment. Additionally, duplicate baseline samples were collected from the scrubber water tank before any etching to account for background PFAS concentrations.

We analyzed the scrubber blowdown and baseline samples for TF, AOF, and 24 target PFASs. The baseline-corrected TF concentrations ranged from below the limit of quantification (<LOQ) to 506 mg/L, while the AOF concentrations from 0.3 to 91 µg F/L. Summed concentrations of target PFASs ranged from 0.02 to 3.4 µg/L for the baseline samples and from 0.2 to 12.8 µg/L in the post-etching samples (Figure 2). Perfluorocarboxylic acids (PFCAs), a PFAS class of regulatory concern, dominated the target PFAS profiles in all etching-related scrubber samples, comprising over 94% of the total target PFASs. Target PFASs accounted for 8-32% of the total AOF in the samples, suggesting the presence of additional unidentified organofluorine compounds (Table 1). These findings highlight the role of plasma etching processes as a source of organofluorine compound in fab emissions.

Conclusions and Future Steps:

We conclude that (1) PFASs are formed during plasma etching processes and are captured in the scrubber blowdown from exhaust gases; and (2) target PFASs quantified in these samples can only explain up to 32% of the total AOF. Future steps will focus on: (1) conducting nontarget PFAS analysis in an effort to identify other PFASs that explain the remaining portion of the total AOF; (2) determining a more stable baseline between etching experiments; (3) conducting more etching experiments while modifying process variables such as testing other photoresist formulations and utilizing the new Oxford Cobra etcher.

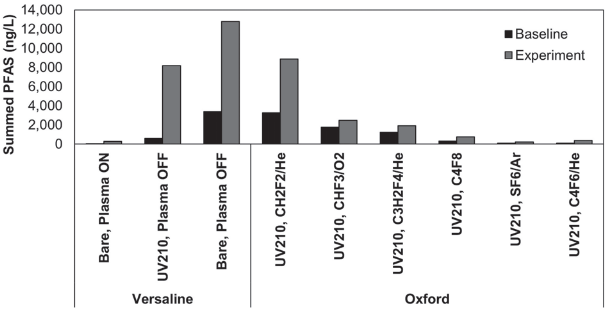

Figure 2: Summed PFAS concentrations for each etching experiment. "Baseline" refers to the sample before etching and "experiment" to the samples collected after etching experiments.

Sample Name	Etcher	PR, Plasma, Gas	AOF (μgF/L)	ΣPFAS (μgF/L)	ΣF in target PFAS (μg F-/L)	% Unexplained	% Explained
3a	Versaline	Bare, Plasma ON	<LOQ	0.27	0.18		
7a		UV210, Plasma OFF	61.97	7.57	5.17	92%	8%
9a		Bare, Plasma OFF	91.07	90.93	9.44	90%	10%
11a	Oxford	UV210, CH2F2/He	13.74	5.62	3.86	72%	28%
13a		UV210, CHF3/O2	2.19	0.70	0.48	78%	22%
16a		UV210, C3H2F4/He	1.79	0.70	0.47	74%	26%
18a		UV210, C4F8	1.32	0.44	0.29	78%	22%
20a		UV210, SF6/Ar	0.27	0.13	0.09	68%	32%
22a		UV210, C4F6/He	1.96	0.29	0.20	90%	10%

Table 1: Summary results for AOF and target PFASs in scrubber blowdown samples from the CNF.

References:

[1] Wang, Z.; DeWitt, J. C.; Higgins, C. P.; Cousins, I. T. A Never-Ending Story of Per- and Polyfluoroalkyl Substances (PFASs)? Environ Sci Technol 2017, 51 (5), 2508–2518. https://doi.org/10.1021/acs.est.6b04806.

[2] Ober, C. K.; Käfer, F.; Deng, J. Review of Essential Use of Fluorochemicals in Lithographic Patterning and Semiconductor Processing. Journal of Micro/Nanopatterning, Materials, and Metrology 2022, 21 (01). https://doi.org/10.1117/1.JMM.21.1.010901.

[3] Jacob, P.; Barzen-Hanson, K. A.; Helbling, D. E. Target and Nontarget Analysis of Per- and Polyfluoralkyl Substances in Wastewater from Electronics Fabrication Facilities. Environmental Science & Technology 2021, 55 (4), 2346–2356. https://doi.org/10.1021/acs.est.0c06690.

[4] Jacob, P.; Helbling, D. E. Exploring the Evolution of Organofluorine-Containing Compounds during Simulated Photolithography Experiments. Environmental Science & Technology 2023, 57 (34), 12819–12828. https://doi.org/10.1021/acs.est.3c03410.

[5] Windsor, A. J.; Clark, J. C.; McMurdy, G.; Joseph, E. A.; Syvret, R. G.; Olson, R. J.; Cha, J. J. Viability of HFO-1234ze(E) (Trans -1,3,3,3-Tetrafluoropropene) as a Low Global Warming Potential Silicon Dioxide Etch Gas. Journal of Vacuum Science & Technology B 2025, 43 (2). https://doi.org/10.1116/6.0004194.

New High Resolution Resists for EUV Lithography

CNF Project Number: 3137-23
Principal Investigator(s): Christopher Kemper Ober
User(s): Dr. Madan Rajendra Biradar, Dr. Gokhan Sagdic

Affiliation(s): Department of Materials Science and Engineering, Cornell University

Primary Source(s) of Research Funding: DuPont and SK hynix Inc.

Contact: cko3@cornell.edu, mrb348@cornell.edu, gs767@cornell.edu

Research Group Website: https://ober.mse.cornell.edu/index.html

Primary CNF Tools Used: ASML PAS 5500/300C DUV Wafer Stepper, JEOL 6300 E-Beam Lithography, P10 Profilometer, Optical Microscope, Veeco Icon Atomic Force Microscope

Abstract:

The semiconductor industry relies heavily on photoresists for fabricating advanced chips. With the growing need for higher resolution and pattern fidelity, EUV lithography presents unique challenges due to the limited number of EUV photons. This necessitates the use of highly sensitive resists such as chemically amplified resists (CAR) and novel double amplification resists (DAR). In DAR systems, ionizing radiation activates photoacid generators (PAGs), which produce acids that depolymerize the polymer backbone into monomers. Each acid can trigger multiple depolymerization events, enabling a double amplification effect. Due to their higher sensitivity of DAR resists compared to CAR, DAR systems require precisely tuned PAGs to control depolymerization kinetics. To address this, we designed and synthesized non-ionic PAGs to be utilized with DAR resists. This report details the design and synthesis of these PAGs and demonstrates their performance with Br-PPA polymer using DUV lithography. The resulting patterns were characterized by AFM microscopy.

Summary of Research:

To fabricate high-performance integrated circuits, the semiconductor industry relies heavily on chemically amplified resists (CARs), which typically comprise a polymer resin, a photoacid generator (PAG), a quencher, and various additives. [1]Most commercial CAR formulations use ionic PAGs because of their high sensitivity and efficient acid generation.[2-3]However, to meet the evolving demands for finer resolution and greater pattern fidelity, there is a growing need to develop next-generation high-performance resist systems. Polyphthalaldehyde (PPA) based resists belong to the class of double amplification resists (DARs), having self-immolative nature.[4-5]Upon acid activation, the polymer undergoes complete depolymerization into monomers, enabling sharp pattern formation and providing an efficient amplification mechanism, as illustrated in Figure 1. However, the higher sensitivity of DAR systems demands the use of optimized PAGs. [6]Non-ionic PAGs have gained importance due to their improved solubility in organic solvents, superior thermal stability during pre- and post-exposure bake steps, and reduced dark loss. By advancing both Br-PPA polymers and non-ionic PAG formulations, it is possible to achieve significant improvements in the performance of next-generation EUV photoresists.

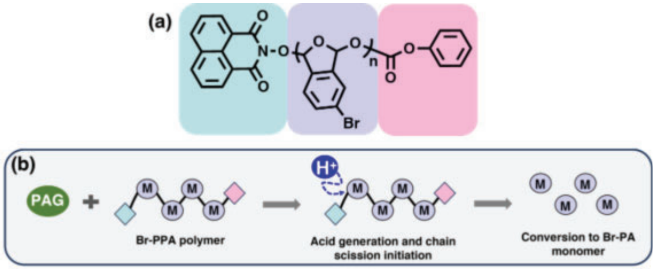

Figure 1: (a) Molecular design of Br-PPA polymer; (b) depolymerization mechanism of Br-PPA resist.

Results and Discussion:

Different functionalized non-ionic PAGs were designed using computational chemistry, synthesized, and characterized by ^{1}H and ^{13}C NMR spectroscopy. Br-PPA polymer was also synthesized and confirmed by ^{1}H NMR. Gel permeation chromatography was used to determine the molecular weight of polymer. A resist formulation, consisting the Br-PPA polymer and 20 wt% PAG in cyclohexanone, was spin-coated onto silicon wafers (2000 rpm, 60 s). These wafers were exposed to DUV radiation using an ASML PAS 5500/300C DUV wafer stepper. Further, pre- and post-exposure baking (90°C), followed by development in isopropyl alcohol (60 s) yielded line-space patterns, which were analysed by using atomic force microscopy as shown in Figure 2. The initial testing of a non-ionic PAG and Br-PPA as DAR resist yielded promising results, demonstrating

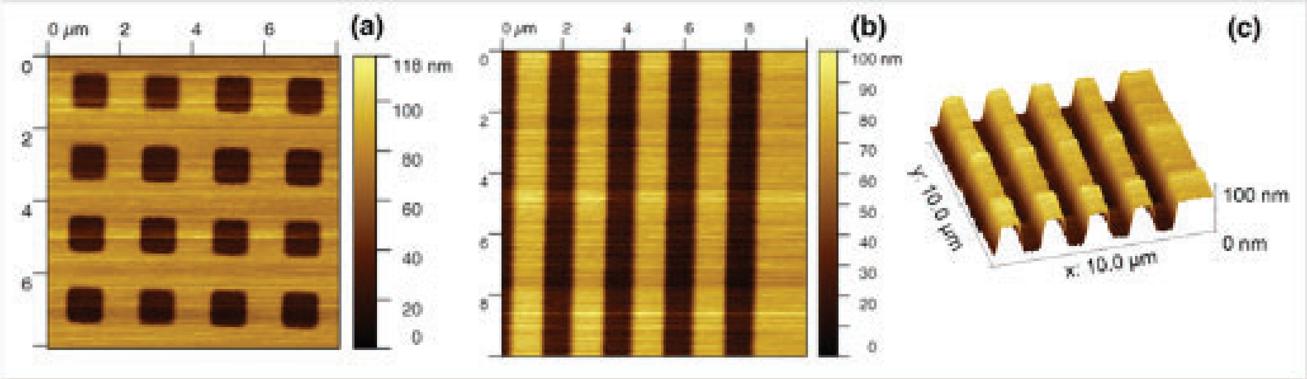

Figure 2: AFM images of 1 µm x 1 µm square hole pattern for DAR resist (a); 1 µm line patterns for DAR resist (b); (c) 3D height image of (b).

the fabrication of 1 µm × 1 µm square hole and line patterns.

Conclusions and Future Steps:

In this work, we developed a series of non-ionic PAGs incorporating various functional groups to evaluate their acid generation efficiency, sensitivity, and acid diffusion behavior, which are key factors affecting overall resist performance. DUV lithography experiments were conducted to evaluate the patterning performance of the DAR resists, and characterized by using AFM and SEM imaging. Further optimization studies, along with E-beam and EUV lithography evaluations, are currently in progress.

References:

[1] Cen, J.; Deng, Z.; Liu, S. Emerging Trends in the Chemistry of Polymeric Resists for Extreme Ultraviolet Lithography. Polym. Chem., 2024, 15 (45), 4599–4614. https://doi.org/10.1039/d4py00957f.

[2] Crivello, J. V. Cationic Polymerization — Iodonium and Sulfonium Salt Photoinitiators. Advances in Polymer Science, 1–48. https://doi.org/10.1007/bfb0024034.

[3] Komoto, K. Photopolymerization of Vinyl Ether by Hydroxy- and Methylthio-Alkylphosphonium Salts as Novel Photocationic Initiators. Polymer, 1994, 35 (1), 217–218. https://doi.org/10.1016/0032-3861(94)90077-9.

[4] Snyder, R.; Baranowsky, P.; Flajslik, K.; Kang, D.; Li, M.; Litchfield, B.; Yamada, S.; Zhang, W.; Oh, K. H.; Ban, C.; et al. Next-Generation EUV Photoresists-Based on Chain-Unzipping Polymers. Advances in Patterning Materials and Processes XLII, 2025, 5. https://doi.org/10.1117/12.3050849.

[5] Deng, J.; Bailey, S.; Jiang, S.; Ober, C. K. Modular Synthesis of Phthalaldehyde Derivatives Enabling Access to Photoacid Generator-Bound Self-Immolative Polymer Resists with Next-Generation Photolithographic Properties. J. Am. Chem. Soc., 2022, 144 (42), 19508–19520. https://doi.org/10.1021/jacs.2c08202.

[6] Biradar, M. R.; Oh, K. H.; Ban, C.; Kim, J. H.; Snyder, R.; Li, M.; Hernandez, K.; Kiliclar, H. C.; Sagdic, G.; Ober, C. K. Non-Ionic Photo-Acid Generators for next-Generation EUV Photoresists. Advances in Patterning Materials and Processes XLII, 2025, 73. https://doi.org/10.1117/12.3050818.